Journal of Physics D: Applied Physics

PAPER

Elastic support of magnetic fluids bearing

To cite this article: Zhuang Wang *et al* 2017 *J. Phys. D: Appl. Phys.* **50** 435004

IOP Publishing Journal of Physics D: Applied Physics
J. Phys. D: Appl. Phys. **50** (2017) 435004 (5pp) https://doi.org/10.1088/1361-6463/aa86f9

Elastic support of magnetic fluids bearing

Zhuang Wang, Zhengdong Hu, Wei Huang[1] and Xiaolei Wang

College of Mechanical & Electrical Engineering, Nanjing University of Aeronautics & Astronautics, Nanjing 210016, People's Republic of China

E-mail: huangwei@nuaa.edu.cn

Received 17 May 2017, revised 11 August 2017
Accepted for publication 18 August 2017
Published 5 October 2017

Abstract

In this paper, a kind of gas support generated by the magnetic fluids seal is investigated numerically and experimentally. Theoretical analysis and experimental tests both indicate that the load carrying capacity of the bearing is mainly determined by the sealing capacity of the magnetic fluids. The experiments also reveal that the load capacity may change with the volumes of magnetic fluids and the air sealed by magnetic fluids.

Keywords: load carrying capacity, magnetic fluids, magnetic field distribution

(Some figures may appear in colour only in the online journal)

1. Introduction

Magnetic fluids (MFs) are one of many functional materials, which compose of single-domain magnetic nanoparticles dispersing in a carrier liquid [1]. Brownian motion prevents the particles from settling under gravity, and surfactant is placed around each particle to provide short range steric repulsion between the particles to avoid agglomeration [2]. Owing to a combination of the pronounced magnetic properties and fluidity inhering in classical liquids, MFs have found wide applications in many industrial processes [3–6].

The behaviors of MFs are mainly determined by their magnetic properties. From the basic physical point of view, MFs are interesting because they can interact with a magnetic field to produce a controllable magnetostatic force on the fluid. Physical principles for the magnetostatic force in MFs under the influence of a non-uniform magnetic field were described in detail by Rosensweig [7]. From the fluid mechanical point of view, this kind of magnetostatic force may provide an elastic support or hold a load. The elastic support representing the MFs drop with a magnet inside was investigated numerically by Bashtovoi *et al* [8]. In 2009, the authors' group also carried out research work on the elastic support of MFs. As shown in figure 1, the magnetic field is generated by eight cylindrical NdFeB magnets, with the size of Φ4.0 mm × 4.0 mm, distributed uniformly on a cylinder surface. The magnets are covered by drops of MFs (1 ml). The supporting force of MFs drop was recorded by a force sensor during the plate moving down. The preliminary research results verified that MFs could generate load capacity under an external magnetic field and the force increases with the increase of magnetization of MFs [9].

Besides the magnetostatic supporting, MFs seal may provide the other kind of load carrying capacity [10]. As shown in the upper right of figure 2, a drop of MFs covers an annular magnet, forming a closed liquid ring. If the bottom of the magnet is bonded with a glass substrate, a load carrying capacity might be expected by the air, which is encapsulated and pressurized by the MFs seal. When the force is larger than the supporting element, then the arrangement can cause it to float, which are highly desirable in a lubrication system. In addition, such a construction can also be regarded as a simple elastic supporting stage system, which may play the role of spring or damper.

However, the physical mechanisms governing the elastic support are still ambiguous. Furthermore, how does the volume of the air chamber affect the supporting forces? To address these questions, a simplified model was set up and the carrying capacity of the bearing was analyzed in theory. Meanwhile, experiments were performed to further confirm the existence of the supporting forces. Theoretical and experimental results indicate that such an air cushion structure can produce a load capacity, since the air pressure inside the chamber may be enhanced by applying a vertical load on the stage.

2. Principle analysis

To gain the essential features of such elastic support, a theoretical model was built, as shown in figure 2. Definitions of

[1] Author to whom any correspondence should be addressed.
Yudao street 29#, Nanjing, People's Republic of China.

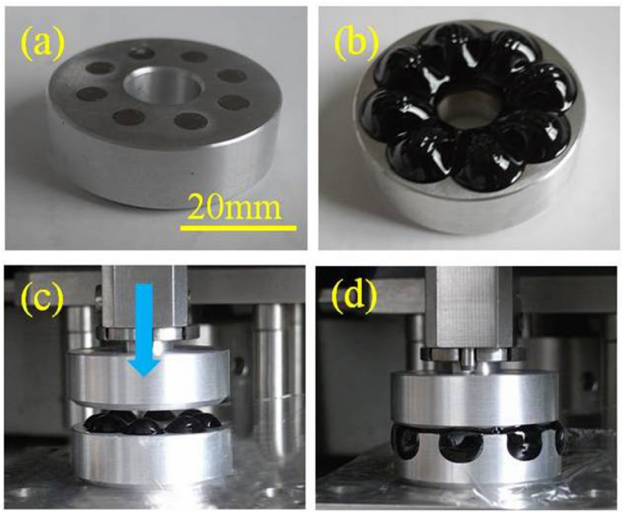

Figure 1. (a) Aluminum cylinder with magnets, (b) cylinder covered with MFs, (c) and (d) supporting force test procedure. [9] Taylor & Francis Ltd. http://tandfonline.com.

the symbols can also be found in figure 2. The magnetization of the MFs interacts with the external magnetic field to produce attractive forces on each magnetic particle. By virtue of the stabilized suspension of the particles in MFs, the attractive magnetic force develops a static pressure inside the fluid. When gravity and surface tension of MFs are ignored, the induced magnetic pressure gradient (∇p) in the fluid can be written as [11, 12]:

$$\nabla p = \mu_0 M \nabla H \tag{1}$$

where μ_0 is the magnetic permeability of free space, M is the magnetization of the MFs and ∇H is the magnetic field gradient. In general, the magnetization M of the MFs is a function of the magnetic field. Since, in practice, a magnetic field in a gap attains 10^5 A m^{-1} and MFs can be regarded as fully saturated (M_s).

Thus, the limiting pressure difference across the MFs seal ($p_i - p_0$) can be calculated as follows [10]:

$$p_i - p_0 = \int_{H_0}^{H_i} \nabla p \cdot \mathrm{d}H = \mu_0 M_s \int_{H_0}^{H_i} \nabla H \cdot \mathrm{d}H = \mu_0 M_s (H_i - H_0) \tag{2}$$

where p_i and p_0 are the hydrostatic pressures on each side of the MFs interface, H_i and H_0 are the corresponding magnetic field intensity magnitudes. The result clearly indicates that only the magnetic field intensities at the fluid-air interface determine the pressure of the enclosed chamber. In this case, the load capacity (F) can be calculated approximately by integrating the pressure over the load carrying surface area ($A_F = \pi r_{\mathrm{in}}^2$). Therefore, the bearing capacity could be written as [10]:

$$F = \int_S (p_i - p_0) \cdot \mathrm{d}A_F = \mu_0 M_s (H_i - H_0) A_F. \tag{3}$$

As can be seen, the bearing capacity mainly depends on the MFs seal. Additionally, the initial factors related to the sealing capacity are the magnetic properties of the MFs and the magnet, as well as the geometry of the bearing.

Possible dynamic supporting process of the bearing could be as follows. When the upper plate just touches the fluid, the air encapsulated by the MFs ring presents no supporting ability, since the magnetic field intensities at the inner and outer fluid interfaces are the same. With the upper plate pressing down, the magnetic field intensity at the inner fluid interface differs from that of the outer. Due to the height between the upper plate and magnet becoming smaller, the inner fluid interface shifts to the position with the higher magnetic field intensity, since when approaching the magnet, the magnetic line becomes dense. On the contrary, for the squeezing action, the intensity of the outer fluid interface wanes, since the outer interface of MFs situates far away from the magnet. Thus, with the height between the plate and magnet decreasing, the magnetic field gradient (∇H between the inner and outer of the fluid interfaces, $H_i - H_0$) grows gradually, and the pressure gradient (∇p) is built up across the MFs seal. As a result, the load carrying capacity (F) increases with the decreasing of the height (h).

3. Experiment and discussion

To further verify the elastic support, a series of experiments are conducted. A N35 NdFeB annular magnet (Φ16 mm $*$ Φ12 mm $*$ 6 mm) with the magnetization in the axial direction was chosen. The bottom of the magnet is connected with a glass without any gas leak.

The Fe_3O_4-based MFs prepared by the co-precipitation technique was used in this paper. To overcome agglomeration, the magnetic particles were coated with succinimide (surfactant) and dispersed in α-olefinic hydrocarbon synthetic oil (carrier liquid). The saturation magnetization of the MFs is about 2.38×10^4 A m^{-1}, corresponding to the particle volume fraction of 6.32%. The image of the MFs absorbed on the magnet was shown in figure 2.

The load carrying capacity of the MFs bearing was measured using a tensile force testing platform, as shown in figure 3. A servo motor connected with a reducer is used as power that drives a transmission screw. A force sensor fixed with the screw can move in a vertical direction. The servo motor is controlled by a servo driver and an NI motion control card. The force sensor is connected with the NI data acquisition card, which can collect the value of force in real time by PC. Thus, the data of the supporting force over the displacement can be recorded. To overcome the slipping, the upper plate is connected mechanically with the force sensor. The center of the force is ensured by a positioning fixture.

The measuring range of the force sensor is 5 N with a resolution of 0.001 N. The transmission accuracy of the screw is 0.01 mm. During the test process, the speed of the force sensor in the vertical direction is fixed at 0.01 mm s^{-1}.

Figure 4 presents the load capacity (F) plotted as function of the height (h). As expected, the supporting force increases with the decrease of the height and the maximum load carrying capacity of the bearing is about 1.1–1.6 N under the three drop volume conditions. Displacement of the upper plate in the axial direction leads to the deformation of the MFs ring. Also,

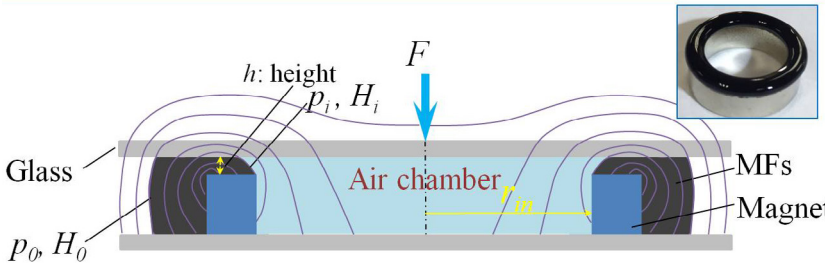

Figure 2. Shematic diagram of the bearing. (The upper right presents a drop of MFs covering on an annular magnet.)

the interface of the outer fluid will overflow in the radial direction, which enhances the ∇H between the inner and outer of the fluid interfaces. Therefore, the induced magnetic pressure gradient (∇p) in the fluid improves, as well as the final load carrying capacity. The smaller the height between the plate and magnet, the greater the aforementioned force.

The load carrying capacity of the numerical simulation was also given in figure 4 and the corresponding description of the numerical model was shown in figure 2. According to equation (3), to obtain the load capacity of the bearing, the magnetic field gradient (∇H between the inner and outer of the fluid interfaces, $H_i - H_0$) becomes the primary problem since μ_0, M_s and A_F are the constants. In this paper, the solution of the problem is done numerically using a magnetic field finite element method (FEM) by Ansoft Maxwell ver. 10.0 software. The input parameters of the geometrical and magnetic are in accordance with the experiments. As mentioned above, a N35 NdFeB annular magnet with the dimensions of Φ16 mm ∗ Φ12 mm ∗ 6 mm was chosen. The magnetic parameters were set as follows: a remanent flux density of $B_r = 1.18$ T, a coercivity of $H_c = -880$ kA m^{-1} and a relative permeability of $\mu_r = 1.1$. Thus, the magnetic field distributions at different heights as a function of the radius can be achieved (see in figure 5). As the upper plate is in a certain height, the volume of the MFs determines the interface position of the fluid, since the volume of the fluid is incompressible. Therefore, the magnetic field intensities at the inner and outer of the fluid interfaces can be obtained according to the shape and location of the drop surface. After that, the load carrying capacity (F) can be calculated according to equation (3).

Compared with the experimental curves, the theoretical data present a similar variation trend for three volume conditions. For example, at the height (h) of 0.08 mm, for the volume of MFs is 1.5 ml, the calculated H_i is 4.6×10^5 A m^{-1} and H_0 is about 7.2×10^4 A m^{-1}. The area the pressure supported $\left(A_F = \pi r_{in}^2\right)$ is 1.13×10^{-4} m^{-2}, and μ_0 ($4\pi \times 10^{-7}$ N A^{-2}) is the magnetic permeability of the free space. The saturation magnetization of the MFs is about 2.38×10^4 A m^{-1}. Then, according to equation (3), the calculated load capacity (F) is about 1.33 N and the value is close to the experimental result.

In figure 4, while continue to decrease the height, a dramatic increment of the calculated load capacity appears, which is much higher than the measurements. Since no gas leakage is taken into account during the theoretical analysis, the calculated pressure in the air chamber will increase sharply when the volume of the air chamber decreases. However, during the

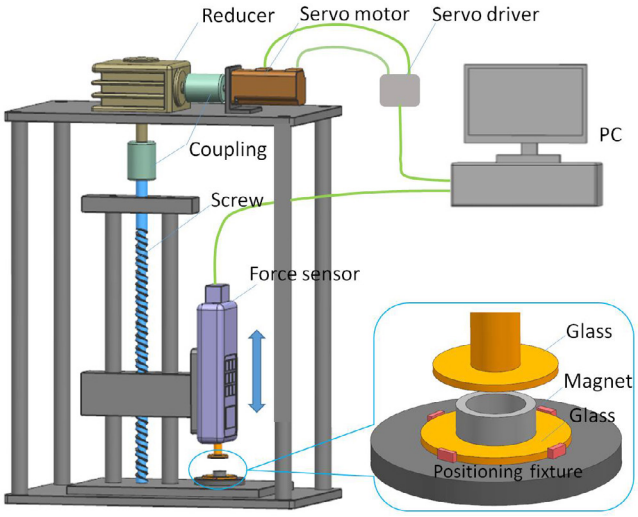

Figure 3. The schematic diagram of the test system.

experimental process, if the upper plate moves down continuously, the resulting pressure increment of the gas would reach the maximum pressure difference that the MFs ring could withstand. Thus, the gas leak is inescapable, especially at the end of the tests. Therefore, the reason why the theoretical data are much higher than the experimental ones at the tiny height might be the gas leakage.

Note that the MFs volume affects the load capacity. Due to the increasing volume of the MFs, the outer fluid interface in the gap will definitely go far away from the magnet in the radial direction, which will further magnify the ∇H between the inner and outer of the fluid interfaces. Thus, the bearing capacity improves as well. Besides, when increasing the volume of MFs, the air encapsulated will also increase. Also, this increased air will also promote the bearing capacity.

Besides the volume of the fluid, the volume of the air chamber also shows obvious effects. Figure 6 presents the load dependency on the original air volume. Although the dosage of MFs is the same, the initial supporting forces appear at different heights. The chamber volume varies greatly among the three bearings. For the bearing with a small gas chamber, a tiny compression of gas volume may cause an obvious pressure increment. Thus, the support force can be detected at a higher position. For the bottom unsealed bearing, the detectible magnetostatic force begins from the lowest height.

In order to consider the effect of the magnetostatic force, the sum of the magnetostatic force and the theoretical values were also given in figure 6. For the bearing filled with hot melt

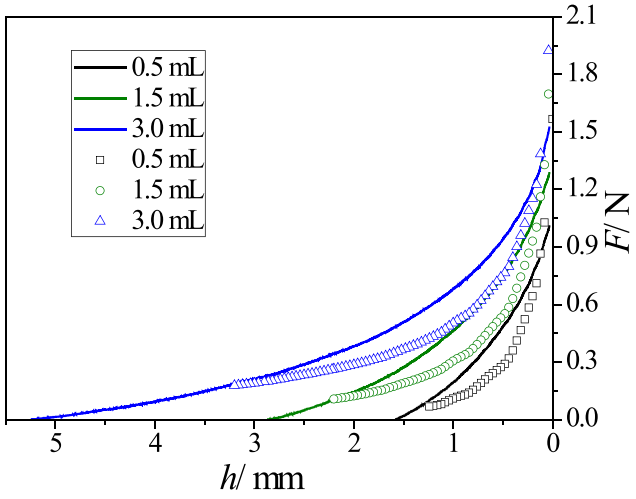

Figure 4. Dependence of the load carrying capacity (F) on the height (h) between the upper plate and the magnet for different drop volumes (lines—the experimental data, dots—theoretical ones).

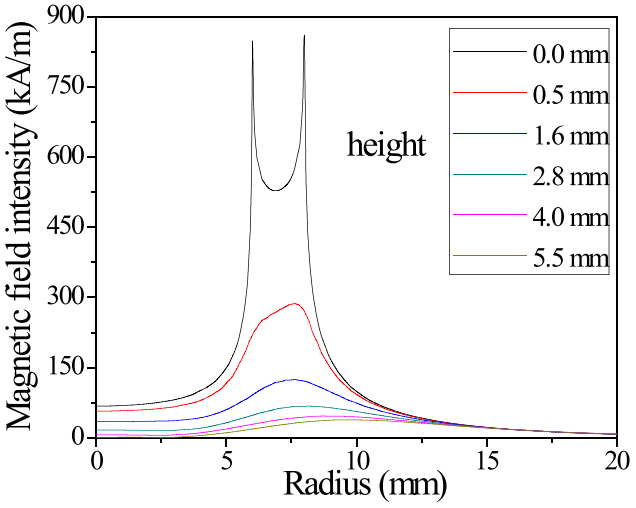

Figure 5. The modeled magnetic field intensity at different heights as a function of the radius for the ring-shaped magnet.

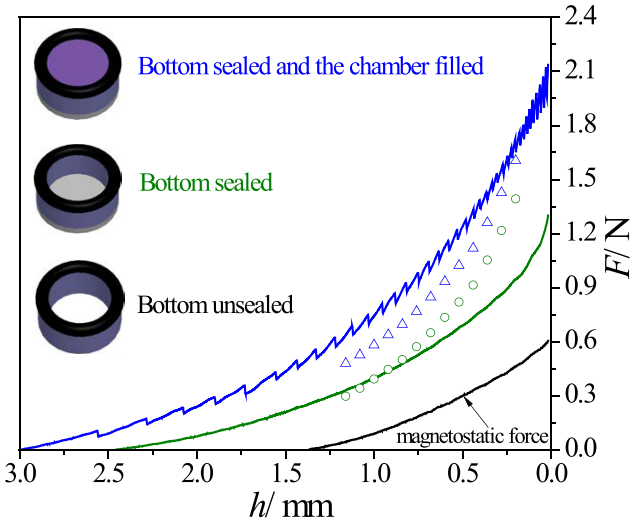

Figure 6. Dependence of load carrying capacity on the original air volume (lines—the experimental data, dots—the sum of the theoretical value and magnetostatic force; the drop volume of MFs is 1.0 ml).

glue, because of the gas leakage (small gas volume condition), the sum of the magnetostatic force and the theoretical value seem to fit the measurements well. It shows that the magnetostatic force plays a leading role for the small chamber condition. When increasing the volume of the gas chamber (only bottom sealed condition), the sum data gravely deviate from the experimental values. The result indicates that the load carrying capacity of the bearing mainly comes from the MFs sealing capacity and the magnetostatic force can be ignored. That is the reason why the magnetostatic force was not considered during the theoretical calculation in figure 4.

Compared with the magnet bottom sealed situation, the lowest supporting force is obtained for the bottom unsealed one. As the chamber of the annular magnet is filled with hot melt glue, the maximum load capacity reaches to 2 N, which is almost 3.5 times higher than the bottom unsealed condition. Such a result further confirms that the gas sealed by MFs helps to improve the supporting force.

According to the ideal gas law, the pressure of gas in a closed container with changing volume is given by:

$$P_2 = \frac{P_1 V_1}{V_2} \tag{4}$$

where P_1 is the initial pressure and V_1 is the initial volume. P_2 is the attainable pressure in the gas chamber. As the upper plate moves down, assuming no gas leak, the pressure may reach the maximum value when the volume of chamber approaches zero, then:

$$P_{2,\max} = \lim_{V_2 \to 0} P_2. \tag{5}$$

When the bottom of the magnet is unsealed, V_2 tends to be infinite and P_2 is the atmospheric pressure. The load acting on the plate is only generated by the magnetostatic force of the MFs. An obvious increment was observed as the bottom of the magnet is bonded with a glass. When the chamber of the annular magnet is occupied, which means V_2 reducing further, the pressure in the chamber shows a rapid increase and the maximum elastic support for static pressure is up to 2.2 N cm^{-2}. So, narrowing the air chamber is an effective way to enhance the bearing capacity.

In addition, the force ripple was observed for the bearing filled with hot melt glue (see figure 6). The original gas volume of the bearing is about 0.339 cm^3, which is much less than the bottom sealed one (1.018 cm^3). Compressing the bearing will cause gas to escape from the seal at an early stage since the pressure in the smaller chamber becomes larger than the pressure that can be counteracted by the MFs seal. In this way, the support force may decline slightly. It should be pointed out that the limiting pressure of the MFs seal is changing at different positions. The smaller the height is, the larger the seal capacity it shows. When the upper plate moves down, the gas continues to be compressed, and the supporting force increases again. On one hand, the discontinuous response of the bearing may decrease the supporting force after gas leak. On the other hand, such discontinuous response may provide a positive way of overload protection, due to gas escaping.

4. Conclusion

In this paper, a type of gas support provided by the MFs seal is studied. Theoretical analyses show that the load carrying capacity of the bearing is mainly determined by the pressure difference across MFs interface. Specific values of the support can be controlled by the geometric and magnetic parameters of MFs and magnet. The experiments reveal that the load capacity of the bearing increases with the increase of the MF volume. Besides, a decrease in the original volume of the gas sealed by MFs helps to improve the elastic support.

As is known, the pressure of the MF seal changes at different height. The smaller the height is, the larger the seal capacity it shows. Therefore, the support force increases with the decreasing of the height. However, the seal capacity cannot withstand a gas support pressure above the final limiting value. From the mechanical point of view, the findings reported in this study will impact upon some important technologies, such as hydrostatic bearing and high precision positioning systems.

Acknowledgments

The authors are grateful for the support provided by the National Natural Science Foundation of China (No. 51475241) and the Fundamental Research Funds for the Central Universities (No. NE2017104).

References

[1] Scherer C and Figueiredo A M 2005 Ferrofluids: properties and applications *Braz. J. Phys.* **6** 718–27
[2] Charles S W 2003 The preparation of magnetic fluids *Lect. Notes Phys.* **594** 3–18
[3] Lebedev A V and Lysenko S N 2009 A multifunctional stabilizer of magnetic fluids *Appl. Phys. Lett.* **95** 013508
[4] Umehara N and Komanduri R 1996 Magnetic fluid grinding of HIP-Si_3N_4 rollers *Wear* **192** 85–93
[5] Shen C, Huang W, Ma G and Wang X 2009 A novel surface texture for magnetic fluid lubrication *Surf. Coat. Technol.* **204** 433–9
[6] Ochonski W 2005 The attraction of ferrofluid bearings *Mach. Des.* **77** 96–9
[7] Rosensweig R E 1997 *Ferrohydrodynamics* (New York: Dover)
[8] Bashtovoi V G, Bossis G, Kabachnikov D N, Krakov M S and Volkova O 2002 Modelling of magnetic fluid support *J. Magn. Magn. Mater.* **252** 315–7
[9] Huang W, Shen C and Wang X 2009 Study on static supporting capacity and tribological performance of ferrofluids *Tribol. Trans.* **52** 717–23
[10] Lampaert S G E, Spronck J W and Ostayen R A J V 2016 Load & stiffness of a planar ferrofluid pocket bearing *The 17th Nordic Symp. on Tribology*
[11] Oldenburg C M, Borglin S E and Moridis G J 2000 Numerical simulation of ferrofluid flow for subsurface environmental engineering applications *Transp. Porous Media* **38** 319–44
[12] Berkovsky B M, Medvedev V F and Krakov M S 1993 *Magnetic Fluids Engineering Applications* (Oxford: Oxford University Press)